JMEPEG (2004) 13:327-334
DOI: 10.1361/10599490419298

1059-9495/$19.00

Chemical Stability of Glass Seal Interfaces in Intermediate Temperature Solid Oxide Fuel Cells

Zhenguo Yang, Guanguang Xia, Kerry D. Meinhardt, K. Scott Weil, and Jeff W. Stevenson

(Submitted 25 November 2003)

In intermediate temperature planar solid oxide fuel cell (SOFC) stacks, the interconnect, which is typically made from cost-effective, oxidation-resistant, high-temperature alloys, is typically sealed to the ceramic positive electrode-electrolyte-negative electrode (PEN) by a sealing glass. To maintain the structural stability and minimize the degradation of stack performance, the sealing glass has to be chemically compatible with the PEN and alloy interconnects. In the present study, the chemical compatibility of a barium-calcium-aluminosilicate (BCAS) based glass-ceramic (specifically developed as a sealant in SOFC stacks) with a number of selected oxidation resistant high temperature alloys (and the yttria-stabilized zirconia electrolyte) was evaluated. This paper reports the results of that study, with a particular focus on Crofer22 APU, a new ferritic stainless steel that was developed specifically for SOFC interconnect applications.

Keywords ferritic stainless steels, interconnect, sealing glass, solid oxide fuel cell

1. Introduction

Solid oxide fuel cells (SOFCs), which convert chemical energy of a fuel to electricity via an electrochemical reaction, have become increasingly attractive to the utility and automotive industries for a number of reasons, including their high efficiency and low emissions. Among the different SOFCs, the planar type, as exemplified in Fig. 1, is expected to be a mechanically robust, high power-density, and cost-effective design. Functionally, the interconnect in a planar SOFC stack acts as a separator plate, physically separating the fuel at the anode side from the air at the cathode side. Thus, to allow the SOFC stack to function well, the interconnect has to be sealed to the adjacent components, such as positive cathode-electrolyte-negative anode (PENs) or metallic frames that hold the PENs. The seals not only prevent mixing of fuel and air, but also keep the fuel from leaking out of the stack. Thus, seal performance not only greatly affects the structural integrity and stability of the stack, but could also dictate the overall stack performance.

With the steady reduction in SOFCs operating temperatures to the intermediate range of 650-800 °C,[1,2] oxidation-resistant, high-temperature alloys have become favorable materials for interconnect components due to their low raw material and manufacturing cost.[3-8] Among these alloys, some cost effective ferritic stainless steels offer good thermal expansion matching to the ceramic PEN in the stacks. Among the ferritic compositions, chromia forming alloys appear more promising than alumina formers mainly due to the higher conductivity of the oxide scale formed on the surface of the alloy during SOFC operation.[9,10] The sealing between stack components is often carried out using a glass-ceramic (i.e., bonding is achieved by heating a glass to a suitable softening point; the glass then devitrifies during SOFC stack operation to form a mixture of crystalline phases), though other sealing technologies are also under consideration by different developers. In order to maintain the structural stability and minimize the degradation of SOFC performance, the sealing materials have to be chemically compatible with the alloy interconnect.

In this study, a barium-calcium-aluminosilicate (BCAS) based glass specifically developed as a sealant in SOFC stacks[11] was chosen as an example. Its chemical compatibility with selected alloy candidates from different groups of traditional oxidation-resistant, high-temperature alloys has been systematically evaluated. Results for several traditional alloys were published previously and the mechanisms regarding the interactions between the sealing glass and alloy interconnects were interpreted as well.[12,13] This paper discusses the chemical stability of BCAS glass-ceramic seal interfaces with YSZ electrolyte and chromia-forming ferritic stainless steels, with particular emphasis on Crofer22 APU, a new ferritic stainless steel that was developed specifically for SOFC interconnect application.[14] For purposes of comparison, the chemical compatibility of the sealing glass with traditional chromia-forming ferritic stainless steels will also be briefly discussed.

2. Experimental

The candidate alloys involved in this study include AL29-4C, 446 and Crofer22 APU. Their chemical compositions are listed in Table 1. Alloy coupons with a thickness of 0.5-1.0 mm were first cut into 12.7 × 12.7 mm squares, and then ground and polished using 600 grit SiC paper. Before joining, the

This paper was presented at the Fuel Cells: Materials, Processing, and Manufacturing Technologies Symposium sponsored by the Energy/Utilities Industrial Sector & Ground Transportation Industrial Sector and the Specialty Materials Critical Technologies Sector at the ASM International Materials Solutions Conference, October 13-15, 2003, in Pittsburgh, PA. The symposium was organized by P. Singh, Pacific Northwest National Laboratory, S.C. Deevi, Philip Morris USA, T. Armstrong, Oak Ridge National Laboratory, and T. Dubois, U.S. Army CECOM.

Zhenguo Yang, Guanguang Xia, Kerry D. Meinhardt, K. Scott Weil, and **Jeff W. Stevenson,** Pacific Northwest National Laboratory, Richland, WA 99352. Contact e-mail: zgary.yang@pnl.gov.

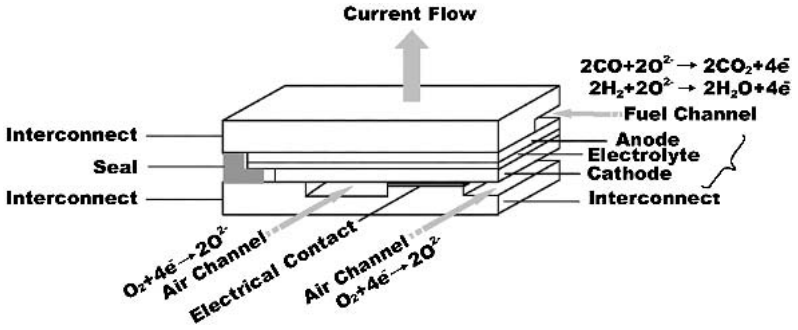

Fig. 1 Schematic illustration of a repeat unit for a "generic" planar solid oxide fuel cell stack

Table 1 Alloy Compositions

Alloys	Cr	Fe	C	Mn	Si	Al	Ti	P	S	Zr	Re
446	25	Balance	0.20	1.50	1.00	…		0.04	0.03	…	…
Fecralloy 22	Balance					5.0	…			0.10	Y
Crofer 22 APU (a)	22.8	Balance	0.005	0.45	…	…	0.08	0.016	0.002	…	0.06 LA
AL29-4C (a)	29.0	Balance	0.01	0.3	0.2	…	…	0.025	0.02	…	…

(a) Crofer and AL are trade marks of ThyssenKrupp and Allegany Ludlum, respectively.

polished alloy coupons were ultrasonicated in alcohol for 10 minutes, and then rinsed with acetone. The electrolyte coupons were made by aqueous tape casting of 8 mol% yttrium-stabilized zirconia (YSZ) obtained from Zirconia Sales (Kennesaw, GA). The tape was formed by mixing an aqueous slurry of zirconia powder with an acrylic emulsion binder (Rohm & Haas, Philadelphia, PA) and cast on a Mylar carrier film to dry. The dry tape was cut into coupons and sintered at 1350 °C. The tape was then cooled and creep flattened at 1350 °C.

The sealing glass, designated as G18, is a BCAS-based glass that has the following composition as analyzed by inductively coupled plasma (ICP): BaO (56.10%), CaO (7.19%), Al_2O_3 (5.39%), B_2O_3 (6.66%), and SiO2 (21.45%). This glass was specifically developed at Pacific Northwest National Laboratory (PNNL, Richland, WA) for SOFC stack sealing applications.[12] In addition to the designated oxide components, analysis also revealed impurities of K_2O (0.26%), Li_2O (0.06%), NiO (0.04%), MgO (0.36%), Na_2O (0.43%), SO_3 (0.25%), SrO (0.11%), Fe_2O_3 (0.05%), Y_2O_3 (0.08%), ZrO_2 (1.56%), and dissolved water. The glass was produced by melting the raw material oxides at 1400 °C for 60 min in a platinum crucible, followed by roller quenching after a temperature reduction to 1250 °C. Oxygen was injected to stir the melt for the duration of the melt time. The glass frit was subsequently dry-milled in an alumina-lined jar with alumina media to <15 μm particle size. The resulting powder was then attrition-milled with zirconia media in isopropanol to an average particle size of 1 μm and dried before tape casting. The 0.8 mm thick tapes were formed from organic-based tape-cast 0.2 mm sheets, which were laminated to the final thickness.

To prepare a joined "couple," the glass tape was sandwiched between two identical alloy coupons or an alloy coupon and YSZ plate, as shown in Fig. 2(a), and then placed into a loading fixture in an electric furnace. A dead load of 6.9×10^3 Pa was applied on top of the joints. The joining was carried out by heating in air to 850 °C for 1 h, followed by a dwell at 750 °C for a designated period of time before cooling. During the heat treatment the glass softened and bonded to the alloy coupons and YSZ electrolyte. As some devitrification (formation of crystalline species) also occurred during the heat treatment, the G18 will be referred to as a "glass-ceramic" material. The heating and cooling were controlled at 2 and 1 °C/min, respectively. The couples were subsequently epoxy-mounted and sectioned. Polished cross-sections were examined via scanning electron microscopy (JEOL Model 5900LV) (Peabody, MA) and energy-dispersive x-ray analysis (EDX) at an operating voltage of 20 kV.

3. Results and Discussion

3.1 Interfaces in the Alloy-Glass-YSZ Seal

Through heat treatment in air (850 °C for 1h followed by 750 °C for 4 h), a coupon of AL29-4C was joined to an identically sized YSZ plate by the sealant G18 to form a joined couple, as shown schematically in Fig. 2(a). The joined couple was then cross sectioned at the middle and analyzed by scanning electron microscopy (SEM). A scan of the entire cross-section revealed an inhomogeneous microstructure along the AL29-4C/G18 interface, but a homogeneous one along the G18/YSZ interface. At the edges of the joined couple, it appeared that the AL29-4C reacted with G18 during heating to form a yellowish product ($BaCrO_4$, as discussed in the following section) along the AL29-4C/G18 interface, leading to separation of the sealing glass-ceramic and the stainless steel. In the interior area, as shown in Fig. 2(c), the sealing glass-ceramic appeared to be well bonded to the stainless steel, with a clearly discernible steel/glass-ceramic interface. At this interface, the glass-ceramic interacted with the stainless steel, forming a re-

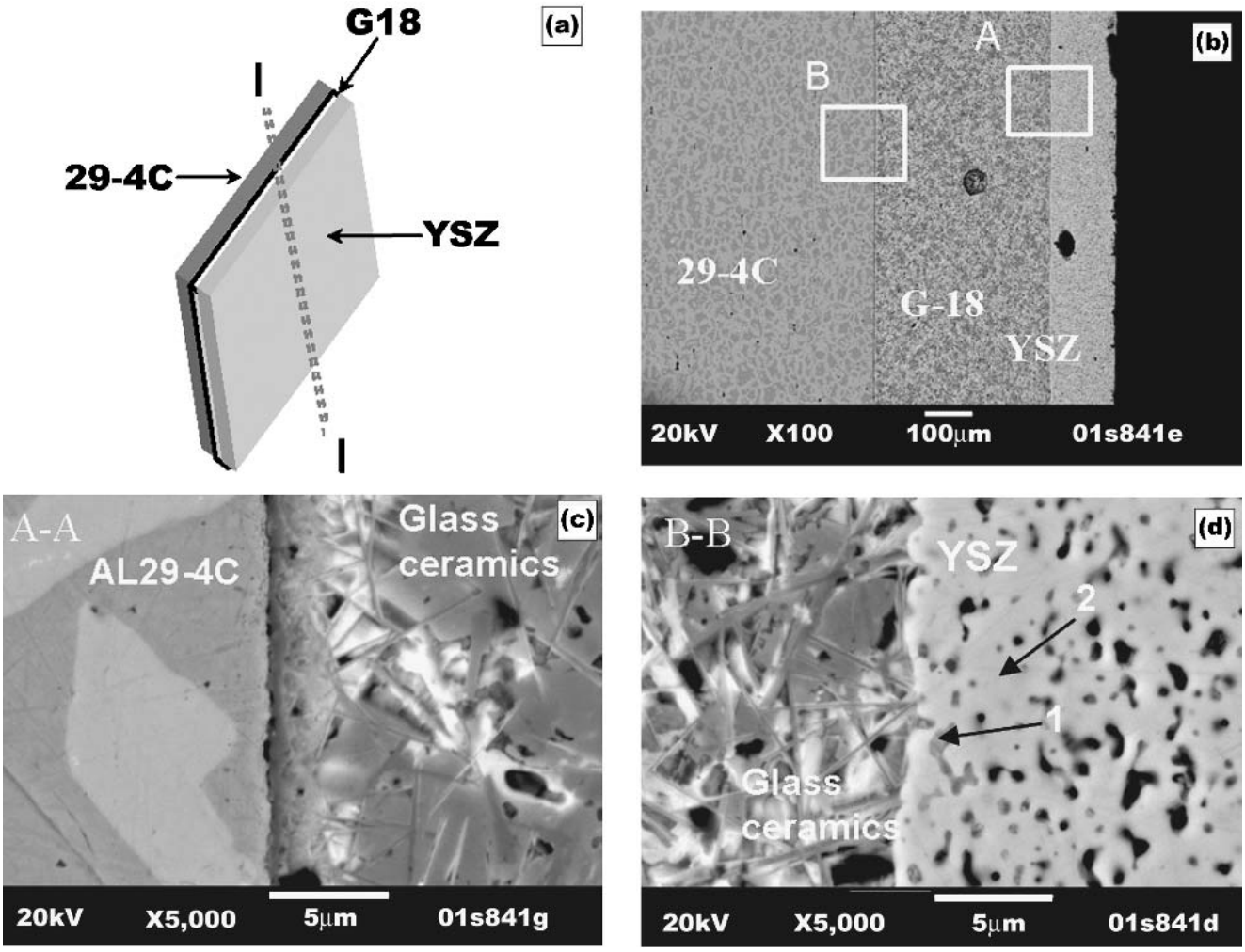

Fig. 2 **(a)** Schematic illustration of a 29-4C/G18/YSZ couple, and SEM images of the interfacial cross section: **(b)** in the interior area, **(c)** from the region marked as B, and **(d)** the region marked as "A" in (b). The 29-4C coupon (12.7 × 12.7 × 0.5 mm) was joined to the YSZ plate (12.7 × 12.7 × 0.5 mm) with G-18 via heat treatment at 850 °C for 1 h, followed by 750 °C for 4 h in air.

action zone (see discussion below). The glass-ceramic was also well bonded to the YSZ along the G18/YSZ interface, as shown in Fig. 2(d), with no significant reaction between the two materials. Some penetration of the glass-ceramic into the YSZ was evident, which likely resulted in strong bonding between the glass-ceramic and the YSZ plate via mechanical interlocking. EDS point analysis (refer to Fig. 2d and Table 2) was used to estimate the glass composition in the pores near the YSZ surface.

Given the fact that the glass-ceramic/alloy interface appeared to be weaker and more complicated than the glass-ceramic/YSZ interface due to the chemical interactions occurring at that interface (and, in some cases, the relatively weak oxide scale adherence to the alloy substrates), the balance of this study focused on glass-ceramic/alloy interfaces.

3.2 Chemical Stability of the Interface between G18 and Traditional Chromia Forming Alloys

The ferritic stainless steel 446 was selected as an example of traditional chromia forming alloys; its chemical stability with the glass-ceramic is briefly discussed here. (A more detailed treatment is available in Ref 12). As schematically shown in Fig. 3(a), two identical 446 coupons were joined by the sealant G18 to form a joined couple via heat treatment in air at 850 °C for 1 h, followed by 750 °C for 4 h. The joined couple was then cross-sectioned at the middle and the interface of the joint was analyzed on SEM. A scan of the entire cross section revealed an inhomogeneous microstructure along the glass/446 interfaces. Accordingly, detailed SEM analysis was carried out on

Table 2 Results of X-Ray Energy Dispersive Analysis at Points Marked in Fig. 2

Elements (atomic%)	O	Al	Si	Ca	Ba	Zr	Y
Point 1	65.99	…	…	…	…	29.29	
						4.72	
Point 2	69.56	0.73	4.24	1.30	4.78	19.39	

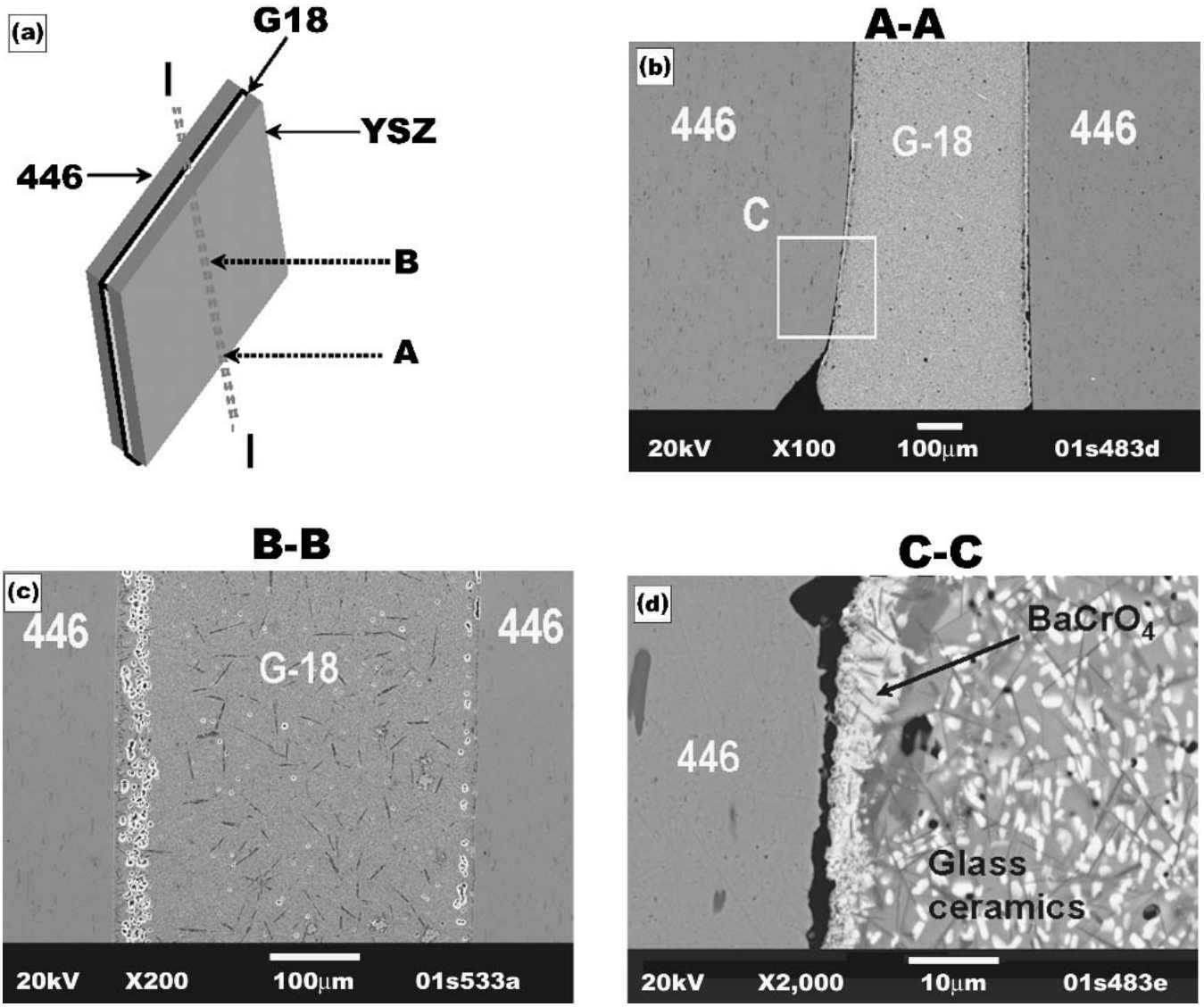

Fig. 3 Interfacial reactions between G18 sealing glass and 446 stainless steel: **(a)** a schematic illustration of the joined couple (446/G18/446), and SEM images of the interfacial cross section at: **(b)** the edge area A, **(c)** the interior region, and **(d)** from the region marked as "C" in (b). The 446 coupons (12.7 × 12.7 × 0.5 mm) were joined to the G18 through heat treatment at 850 °C for 1 h, followed by 750 °C for 4 h in air.

different locations from the edge to the inside area on the interfaces. Figure 2(b) shows a typical secondary electron image taken from the edge area of the joint couples. An enlarged image from the area marked as C is further shown in Fig. 3(d). The images from the edge area clearly indicate that the sealant G18 reacted with the ferritic stainless steel 446 to form a yellowish compound, creating gaps between the glass-ceramic and stainless steel coupons after heat treatment. Detailed structural and chemical analyses[12] confirmed that the formed compound was barium chromate ($BaCrO_4$) that evolved from a reaction between the barium oxide in G18 and the chromia scale grown on chroming forming alloys during heating via the following reaction:

$$2Cr_2O_3\ (s) + 4BaO\ (s) + 3O_2\ (g) = 4BaCrO_4\ (s) \qquad \text{(Eq 1)}$$

The fact that this reaction requires the presence of oxygen or air explains why the $BaCrO_4$ was found only at the edge or near the edge areas of the joint, where oxygen in the air was easily accessible. Due to the large thermal expansion mismatch between $BaCrO_4$ and G18 or 446,[12,15] the extensive formation of $BaCrO_4$ probably resulted in the observed gap between the sealing glass and alloy coupons.

In addition to the above solid-state $BaCrO_4$ formation reaction, the dominant chromia vapor species when moisture is present, chromium oxyhydroxide $[CrO_2(OH)_2]$,[16-18] can also react with barium oxide in the sealing glass to form $BaCrO_4$ via the following reaction:

$$CrO_2(OH)_2\ (g) + BaO\ (s) = BaCrO_4\ (s) + H_2O\ (g) \qquad \text{(Eq 2)}$$

This reaction mechanism helps explain the observed ho-

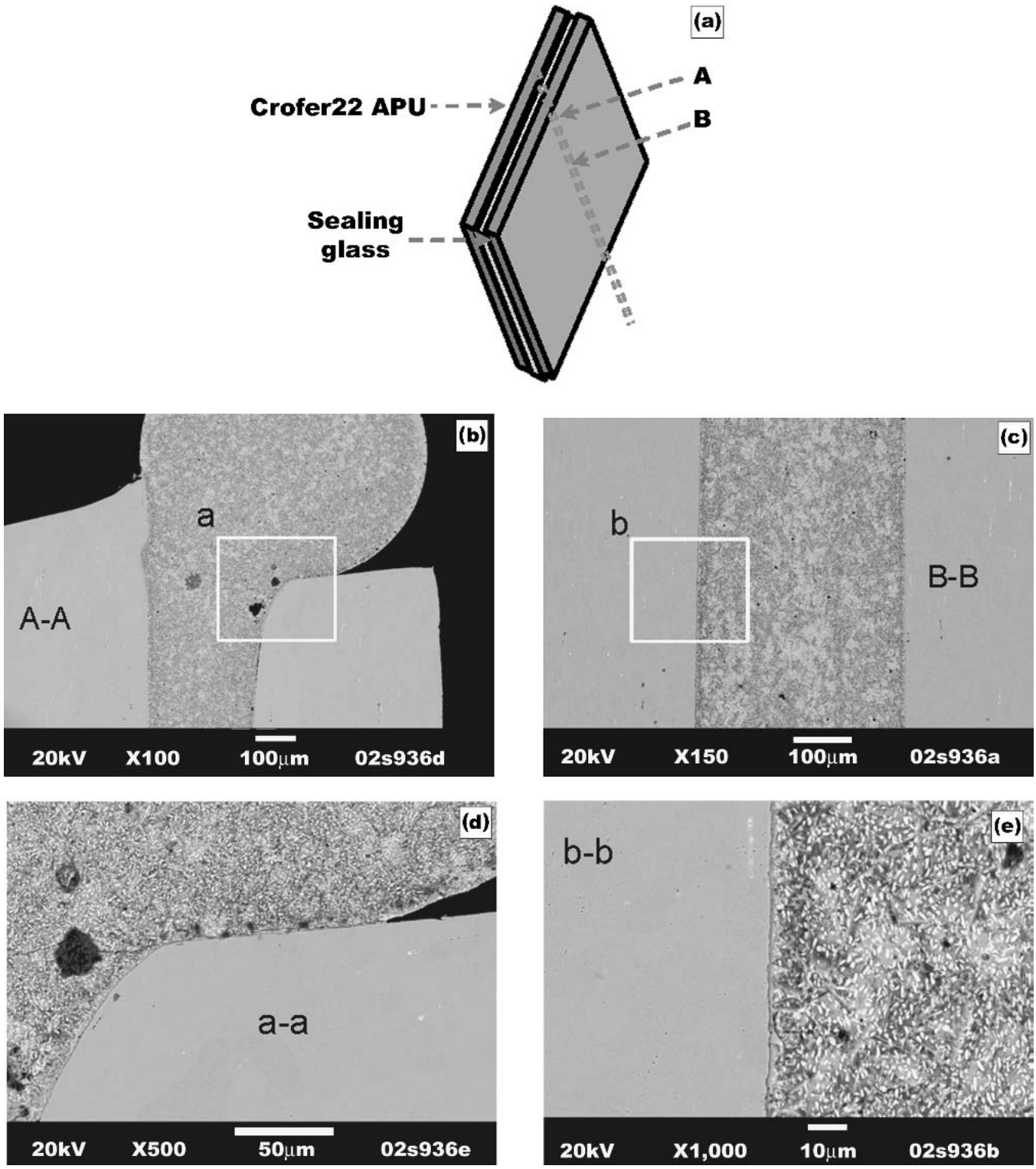

Fig. 4 Interfacial reactions between G18 sealing glass and stainless steel Crofer22 APU: **(a)** a schematic illustration of the joined "couple" (Crofer22 APU/G18/Crofer22 APU), and secondary electron SEM images of the interfacial cross section at: **(b)** the edge area A, **(c)** at the interior region B, **(d)** from the region marked as a in (b), and **(e)** from the region marked as b in (c). The Crofer22 APU coupons (12.7 × 12.7 × 1.0 mm) were joined with G18 through heat treatment in air at 850 °C for 1 h, followed by 750 °C for 4 h.

mogenous $BaCrO_4$ formation on the surface of the glass-ceramic that was squeezed out during the joining heat treatment.

In the interior of 446/G18/446 joint, as shown in Fig. 3(c), there was no $BaCrO_4$ formation, and the sealing glass was bonded to the ferritic stainless steel. A Cr-rich layer was ob-

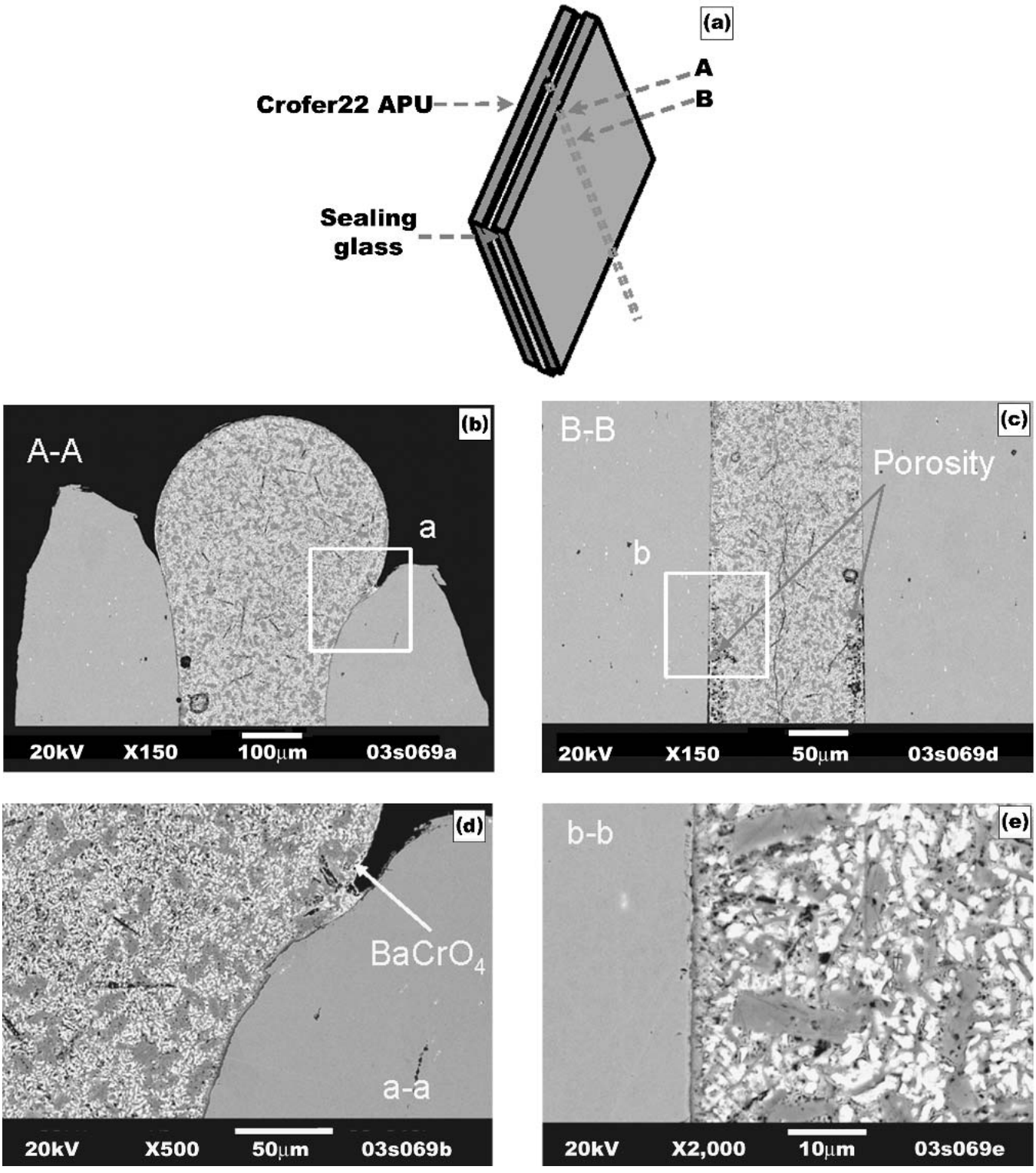

Fig. 5 Interfacial reactions between G18 sealing glass and stainless steel Crofer22 APU: **(a)** a schematic illustration of the joined "couple" (Crofer22 APU/G18/Crofer22 APU), and secondary electron SEM images of the interfacial cross section at: **(b)** the edge area A, **(c)** at the interior region B, **(d)** from the region marked as a in (b), and **(e)** from the region marked as b in (c). The Crofer22 APU coupons (12.7 × 12.7 × 1.0 mm) were joined with G18 through heat treatment in air at 850 °C for 1 h, followed by 750 °C for 24 h.

served in the glass-ceramic at the interface, presumably due to dissolution of Cr from the alloy scale into the glass-ceramic to form Cr-rich phases. The G18/446 interface in the interior area was also characterized by the formation of porosity along the interface, as shown in Fig. 2(c). These pores were likely created through the formation of vapor species via the interaction

of alloy elements, especially Cr, with dissolved water and alkaline oxide residues in the glass.[13]

3.3 Chemical Stability of the G18/Crofer22 APU Interface

A recently developed SOFC interconnect alloy, Crofer22 APU, was investigated for its chemical compatibility with the sealing glass under different thermal histories. Figure 4(a) shows the Crofer22 APU/G18/Crofer22 APU join after heat-treatment under the same thermal condition as for 446, i.e., in air at 850 °C for 1 h, followed by 750 °C for 4 h. The SEM images from the edge and interior areas on the cross section of the joint are presented in Fig. 4(b) and (c), respectively. The areas marked as a in Fig. 4(b) and b in Fig. 4(c) are further enlarged in Fig. 4(d) and (e), respectively. It appeared that the microstructure of the Crofer22 APU/G18 interface was generally homogenous over the entire cross section of the joint. Even at the edge area, the sealing glass-ceramic was well bonded to the stainless steel, and no gap or extensive interaction between the sealing glass and the steel occurred. In the interior, the sealing glass was adherent to the steel, and again no extensive interaction or porosity were observed along the Crofer22 APU/G18 interface. Thus, in comparison with 446, Crofer22 APU demonstrates an improved chemical compatibility with the sealing glass. This is due to the growth of a unique scale on Crofer22 APU during heat treatment, which is comprised of a $(Mn,Cr)_3O_4$ spinel top layer and chromia-rich sublayer.[14,19] The formation of a $(Mn,Cr)_3O_4$ spinel top layer mitigates the direct reaction of sealing glass with chromia and its vapor species.

To further examine the chemical stability between Crofer22 APU and G18, two Crofer22 APU coupons were joined with G18 (see Fig. 5a) in air at 850 °C for 1 h followed by heat treatment at 750 °C for 24 h (instead of the previous 4 h). After the longer heat treatment, it was found that the glass-ceramic squeezed out during joining had turned light yellow. The sealing glass appeared to still be well bonded to the Crofer22 APU, as shown in Fig. 5(b) and (d), which is an enlargement of the area marked as a in Fig. 5(b). Detailed analysis, however, indicated that a detectable amount of $BaCrO_4$ had formed both on

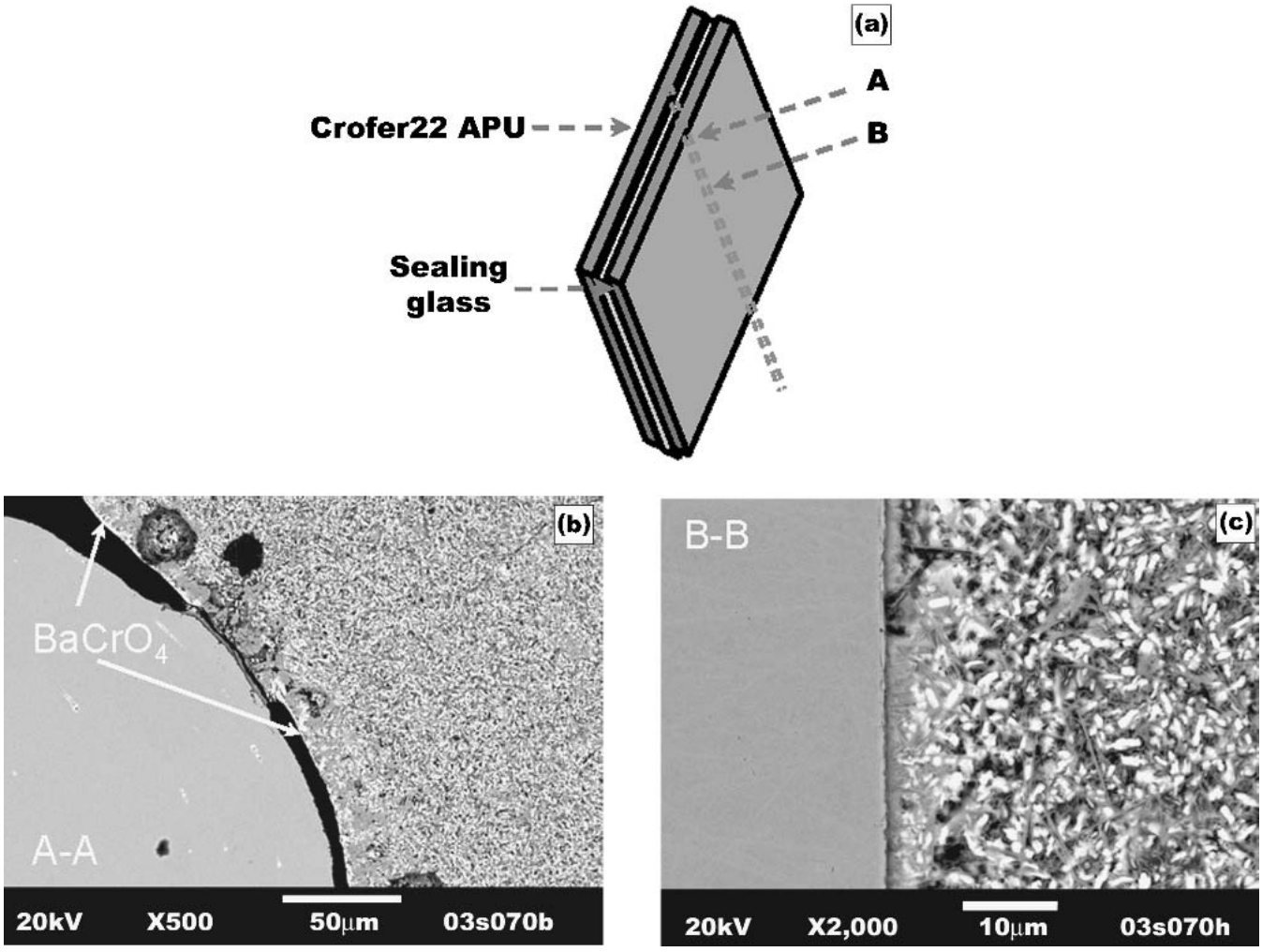

Fig. 6 Interfacial reactions between G18 sealing glass and stainless steel Crofer22 APU: **(a)** a schematic illustation of the joined "couple" (Crofer22 APU/G18/Crofer22 APU), and secondary electron SEM images of the interfacial cross section at: **(b)** the edge area A, and **(c)** at the interior region B. The Crofer22 APU coupons (12.7 × 12.7 × 1.0 mm) were joined with G18 through heat treatment in air at 850 °C for 1h, followed by 750 °C for 168 h (one week).

the surface of the squeezed-out glass ceramic and along the interface at the edge area. Away from the edge area, porosity was evident in the interior of the joint, as shown in Fig. 5(c). The enlarged image in Fig. 5(e) further reveals the porosity and the microstructure of the Crofer22 APU/G18 interface. In a subsequent test, two Crofer22 APU coupons were joined using the sealant G18 at 850 °C for 1 h followed by heat treatment at 750 °C for 168 h (one week). Interfacial microstructures from the edge and interior areas of the joint after this prolonged heat treatment are shown in Fig. 6(a), 6(b), and (c), respectively. Once again, the glass-ceramic squeezed out between the two Crofer22 APU coupons during joining and turned yellow, indicating extensive formation of $BaCrO_4$. At the edge area, the sealing glass was separated from the ferritic stainless steel and $BaCrO_4$ was also observable. In the interior, extensive porosity was found along the Crofer22 APU/G18 interface, although the sealing glass was still bonded to the stainless steel.

Thus, as evidenced by the prolonged test, Crofer22 APU, like the other ferritic stainless steels, reacts with the sealing glass to form $BaCrO_4$ and interfacial porosity, although the kinetics of the interactions appear to be hindered due to the growth of a unique scale on that steel during heat treatment.

4. Conclusions

This work leads to the following conclusions.

The BCAS sealing glass-ceramic interacts with both the YSZ electrolyte and ferritic stainless steel interconnects. Overall, the YSZ electrolyte demonstrates good chemical compatibility and bonding to the glass-ceramic through limited reaction as well as good wetting that leads to the penetration of glass-ceramic into any available open porosity in the YSZ electrolyte. In contrast, the stainless steel interconnect reacts extensively with the sealing glass-ceramic resulting in an interface that is more prone to defects.

For traditional chromia forming stainless steels, the extent and nature of their interaction with the glass-ceramic depends on the exposure conditions and/or proximity of the interface of sealing glass and ferritic stainless steel to the ambient air. At or near the edges, where oxygen from the air is accessible, the chromia scale grown on the steel and its vapor species react with BaO in the glass-ceramic, leading to the formation of $BaCrO_4$. In interior regions where the oxygen or air access is blocked, Cr or chromia dissolves into the BCAS sealing glass to form Cr-rich solid solutions. The stainless steel also react with residual species in the sealing glass-ceramic to generate porosity in the glass-ceramic along the interface in the interior regions.

In comparison with traditional chromia forming stainless steels, the newly developed ferritic stainless steel Crofer22 APU exhibits improved chemical compatibility and bonding with the BCAS based-glass ceramics due to the growth of a unique scale on the alloy during high temperature exposures. Under prolonged heating, however, the alloy still visibly reacts with the sealing glass-ceramic, leading to the formation of $BaCrO_4$ at the edge areas of the joints, solid solution phases, and porosity in the interior regions.

Acknowledgments

The authors would like to thank Nat Saenz, Shelly Carlson, and Jim Coleman for their assistance in metallographic and SEM sample preparation and analysis. The work summarized in this paper was funded as part of the Solid-State Energy Conversion Alliance (SECA) Core Technology Program by the U.S. Department of Energy's National Energy Technology Laboratory (NETL). PNNL is operated by Battelle Memorial Institute for the U.S. Department of Energy under Contract DE-AC06-76RLO 1830.

References

1. B.C.H. Steele and A. Heinzel: "Materials for Fuel Cell Technologies," *Nature,* 2001, *414,* pp. 345-52.
2. N.Q. Mihn: "Ceramic Fuel Cells," *J. Am. Ceram. Soc.,* 1994, *76,* pp. 563-88.
3. K. Huang, P.Y. Hou, and J.B. Goodenough: "Characterization of Iron-Based Alloy Interconnects for Reduced Temperature Solid Oxide Fuel Cells," *Solid State Ionics,* 2000, *129,* pp. 237-50.
4. W.J. Quadakkers, T. Malkow, J. Piron-Abellan, U. Flesch, V. Shemet, and L. Singheiser, in *Proceedings of the 4th European Solid Oxide Fuel Cell Forum,* Vol 2., A. McEvoy, ed., European SOFC Forum, Switzerland, 2000, pp. 827-36.
5. J. Piron-Abellan, V. Shemet, F. Tietz, L. Singheiser, and W.J. Quadakkers, in *Proceedings of the 7th International Symposium on Solid Oxide Fuel Cells,* Vol. 2001-16, H. Yokokawa and S.C. Singhal, ed., The Electrochemical Proceedings Series, Pennington, NJ, 2001, pp. 811-19.
6. S.P.S. Badwal, R. Bolden, and K. Foger, in *Proceedings of the 3rd European Solid Oxide Fuel Cell Forum,* Vol. 1, Ph. Stevens, ed., the European SOFC Forum, Switzerland, 1998, pp. 105-14.
7. T. Brylewski, M. Nanko, T. Maruyama, and K. Przybylski: "Application of Fe-16Cr Ferritic Alloy to Interconnector for a Solid Oxide Fuel Cell," *Solid State Ionics,* 2001, *143,* pp. 131-50.
8. Z.G. Yang, K.S. Weil, D.M. Paxton, and J. W. Stevenson: "Selection and Evaluation of Heat Resistant Alloys for Solid Oxide Fuel Cell Interconnect Applications," *J. Electrochem. Soc.,* 2003, *150,* pp. 1188-1201.
9. P. Kofstad, *Nonstoichometry, Diffusion and Electrical Conductivity in Binary Metal Oxides*, Wiley-Interscience, New York, 1972.
10. P. Kofstad and R. Bredesen: "High Temperature Corrosion in SOFC Environments," *Solid State Ionics,* 1992, *52,* pp. 69-75.
11. K.D. Meinhardt, J.D. Vienna, T.R. Armstrong, and L.R. Peterson: "Glass-Ceramic Material and Method of Making," U.S. Patent, No. 6,430,966, 2001.
12. Z. Yang, K.D. Meinhardt, and J.W. Stevenson: Chemical Compatibility of Barium-Calcium-Aluminosilicate-Based Sealing Glasses With Ferritic Stainless Steel Interconnects in SOFCs," *J. Electrochem. Soc.,* 2003, *150,* pp. A1095-1101.
13. Z. Yang, J.W. Stevenson, and K.D. Meinhardt: "Chemical Interactions of Barium-Calcium-Aluminosilicate-Based Sealing Glasses With Oxidation Resistant Alloys," *Solid State Ionics,* 2003, *160,* pp. 213-25.
14. W.J. Quadadakkers, V. Shemet, and L. Lorenz: "Materials Used at High Temperatures for a Bipolar Plate of a Fuel Cell," U.S. Patent, No. 2003059335, 2003.
15. C.W.F.T. Pistorius and M.C. Pistorius: "Lattice Constants and Thermal-Expansion Properties of the Chromates and Selenates of Lead, Strontium and Barium" *Z. Krist,* 1962, *117,* pp. 259-72.
16. Y. Matsuzaki and I. Yasuda: "Dependence of SOFC Cathode Degradation by Chromium-Containing Alloy of Compositions of Electrodes and Electrolytes," *J. Electrochem. Soc.,* 2001, *148,* pp. A126-31.
17. K. Hilpert, D. Das, M. Miller, D.H. Peck, and R. Weib: "Chromium Vapor Species over Solid Oxide Fuel Cell Interconnect Materials and Their Potential for Degradation Processes," *J. Electrochem. Soc.,* 1996, *143,* pp. 3642-47.
18. R. Weib, D. Peck, M. Miller, and K. Hillert: "Volatility of Chromium from Interconnect Material" in *Proceedings of the 17th Riso International Symposium on Materials: High Temperature Electrochemistry: Ceramics and Metals,* F.W. Poulsen, N. Bonanos, S. Linderoth, M. Mogensen, and B. Zachau-Christianen, ed., Denmark, 1996, pp. 479-84.
19. Z. Yang, M.S. Walker, J. Hardy, G. Xia, and J.W. Stevenson: "Structure and Electrical Conductivity of Thermally Grown Scales on Ferritic Fe-Cr-Mn Steel for SOFC Interconnect Applications," submitted to the Journal of Electrochemical Society, 2003.